scientific reports

Check for updates

OPEN

Cannabis smoke extract disrupts trophoblast differentiation and causes mitochondrial dysfunction beyond the effects of Δ9-THC alone

Cristina Monaco[1], Mahek Minhas[1], Tina Podinic[1], Joshua P. Nederveen[1,2], Amica-Mariae Lucas[3], Thane Tomy[3], Gregg T. Tomy[3], Alison C. Holloway[4] & Sandeep Raha[1]✉

Smoking cannabis remains the most common mode of consumption amongst pregnant people, yet the effects on placentation remain poorly understood. While prior studies have focused on exposure to single components of cannabis (i.e., Δ9-THC and CBD), this approach overlooks the complex toxicology and pharmacology of cannabis smoke exposure. In this study, we used an in vitro model of human trophoblast differentiation to investigate the impact of CaSE (cannabis smoke extract) compared to Δ9-THC. We show that CaSE, but not Δ9-THC induces *CYP1A1* expression, a marker of exposure to combustion by-products. CaSE reduced hCG protein levels and *syncytin-1* gene expression, suggesting impaired syncytialization. Lower concentrations of CaSE (1%, 2.5%) elevated reactive oxygen species without impacting membrane potential, whereas higher concentrations (5%, 10%) disrupted mitochondrial respiration, indicating dose-dependent bioenergetic dysfunction. Antioxidant genes, superoxide dismutase 1 and 2, were distinctly altered indicating the divergence in oxidative stress responses. Interestingly, CB1R antagonism rescued the effects of Δ9-THC exposure, but not CaSE-mediated effects on differentiation markers. Since most cannabis users consume cannabis by smoking, and smoke exposure differs from single components (Δ9-THC), it is important that preclinical models consider smoking when evaluating the impacts of cannabis use during pregnancy.

Keywords Cannabis smoke extract, Trophoblast differentiation, Oxidative stress, Mitochondrial dysfunction, Endocannabinoid signaling, Placental development

Despite the growing popularity and availability of various cannabis products, smoke-inhalation remains the preferred method of cannabis consumption amongst pregnant people[1]. Although preclinical and clinical studies have linked prenatal cannabis use and its constituents to adverse outcomes, such as low birth weight, preterm birth, fetal growth restriction and poor neonatal complications, there is still conflicting evidence regarding these outcomes[2–6]. Additionally, there remains uncertainty in the literature largely because human studies are often confounded by polysubstance use, cannabis potency, variations in cannabis cultivars, and the frequency/duration of exposure[7–9].

Cannabis contains over 500 distinct chemical compounds including the highly abundant cannabinoids extracted for human use,Δ9-tetrahydrocannabinol (Δ9-THC) and cannabidiol (CBD)[10,11]. Like tobacco smoke, cannabis smoke also contains a complex mixture of combustion by-products such as polycyclic aromatic hydrocarbons (PAHs), nitrogen oxides, particulate matter and tar[12]. Most pre-clinical studies focus on the effects of individual injections of THC or CBD[5,6,13–16], which may overlook potential complex effects of the other constituents routinely found in *Cannabis*, including the diverse group of phytocannabinoids and terpenes[17] and the combustion by-products.

The adverse outcomes that have been reported with cannabis use during pregnancy such as preterm birth and low birth weight have been linked to placental dysfunction[18]. The chorionic villi of the placenta are the primary sites of materno-fetal nutrient, metabolic and hormonal exchange[19]. These structures are covered by a layer

[1]Department of Pediatrics, Faculty of Health Sciences, McMaster University, 1280 Main St. W., Hamilton, ON L8S 4K1, Canada. [2]Department of Kinesiology, McMaster University, 1280 Main St. W, Hamilton, ON L8S 4K1, Canada. [3]Department of Chemistry, Centre for Oil and Gas Research and Development (COGRAD), University of Manitoba, 586 Parker Building, 144 Dysart Rd., Winnipeg, MB R3T 2N2, Canada. [4]Department of Obstetrics and Gynecology, McMaster University, Hamilton, ON L8S 4K1, Canada. ✉email: rahas@mcmaster.ca

of multi-nucleated syncytiotrophoblast (ST), which continually differentiate and fuse throughout pregnancy from primitive underlying cytotrophoblast (CT) to establish and maintain placental function[20]. Placentae are rich in mitochondria, which serve as key metabolic sensors that support the energy-intensive demands of cellular dynamic processes during pregnancy, including cell commitment and differentiation[21]. Previously, our research group has demonstrated that exposure to Δ9-THC and CBD in vitro disrupts mitochondrial electron chain function as well as trophoblast fusion in BeWo cells[22,23]. Similarly, animal models of pregnancy with Δ9-THC and/or CBD have also shown placental defects[5,6]. However, recent work has shown differential effects on placental and fetal cytokine and chemokine profiles, as well as on maternal and fetal outcomes when comparing cannabis smoke to injectable forms in a mouse model of pregnancy, suggesting the route of exposure may distinctly impact placental-related outcomes[24,25]. Determining the effects of cannabis smoke on trophoblast syncytialization and overall placental health is crucial in enhancing our understanding of cannabis-induced pregnancy complications whilst considering real-world cannabis usage patterns. Therefore, we hypothesized that THC-dominant cannabis smoke extract (CaSE) would impair trophoblast differentiation and mitochondrial respiration in BeWo b30 cells. We demonstrate that while both CaSE and Δ^9-THC disrupt mitochondrial function and trophoblast differentiation, the mechanism of action may differ between the two exposures. Taken together, these findings underscore the importance of distinguishing between the effects of single components like Δ^9-THC, and the complex mixture of constituents present in cannabis smoke when evaluating risks to placental development and reproductive health.

Results

Cannabis smoke exposure induces CYP1A1, and Δ9-THC is detectable in CaSE-treated cells

To measure Δ9-THC and CBD concentrations in our CaSE, we performed LC-MS/MS on CaSE media before and after 0.22 µm filtration, as well as on cultured cell supernatants collected 48 h post-treatment. Quantification confirmed that following filtration, there was a 48.7 ± 13.0% (mean ± s.d., $n = 3$) reduction in Δ9-THC levels in the media. The post-filtration media contained an equivalent of 224 µM THC (100% CaSE). In sample supernatant of cells treated for 48 h with CaSE, Δ9-THC concentrations were found to be 1.74 µM and 4.30 µM in the 2.5% and 5.0% CaSE, respectively (Fig. 1a, $p < 0.0001$) alongside no substantial detection of CBD levels (Fig. 1b) compared to the vehicle. Representative chromatograms of pre-filtered and post-filtered media as well as sample supernatant can be found in Supplemental Figure S2 (a-c). To assess the extent to which CaSE stimulated genes involved in metabolic and bioactivation pathways, we evaluated gene expression levels involved in the aryl hydrocarbon receptor (AhR) signaling cascade. Gene expression levels of *CYP1A1* (cytochrome P450 family 1 subfamily A member 1), a key enzyme involved in metabolizing PAHs, were upregulated by 900-fold and 1600-fold in 2.5% and 5.0% CaSE, respectively, compared to vehicle (Fig. 1c, $p < 0.0001$). In contrast, Δ9-THC alone did not result in a significant change in the expression of *CYP1A1* (Fig. 1c). LC-MS/MS quantification of cannabinoid metabolites alongside CYP1A1 induction, collectively validated the extent of trophoblast exposure to cannabis smoke constituents.

Cannabis smoke exposure reduces cellular viability along with biochemical markers of trophoblast fusion and differentiation

Treatment of BeWo b30 cells with increasing concentrations of CaSE resulted in a sharp decrease in cellular viability at CaSE concentrations greater than 10% (Supplementary Fig. S1, $p < 0.0001$). At lower dosages of CaSE

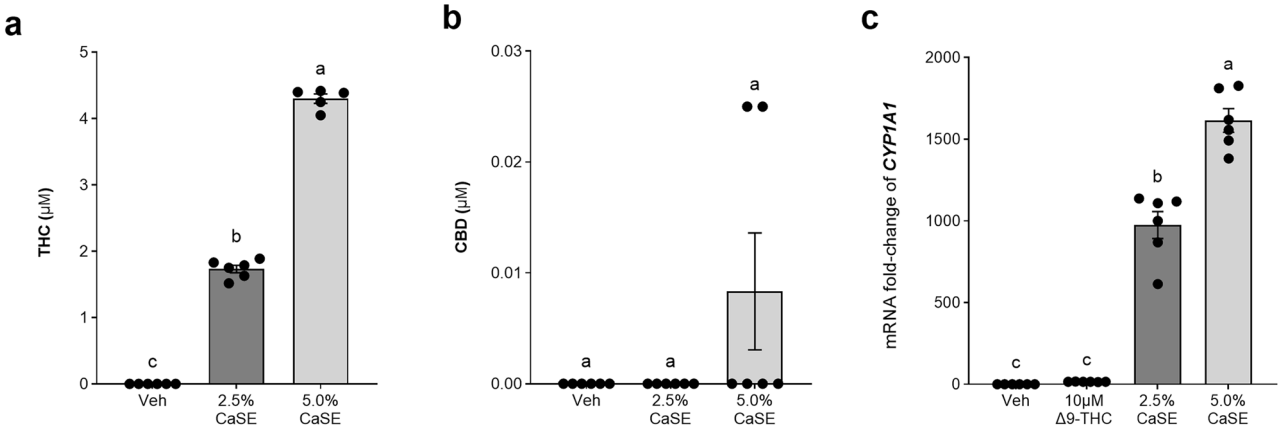

Fig. 1. CaSE induces CYP1A1 expression and contains detectable THC concentrations. BeWo b30 cells were treated with vehicle (0.1% methanol), 10 µM THC, 2.5% or 5.0% CaSE for 48 h during differentiation. (**a**, **b**) Media supernatant was collected 48 h following exposure to CaSE and subjected to LS-MS/MS for metabolite quantification (THC, CBD). The limits of quantitation (LOQ) were 25.3 pg/µL for THC and 23.5 pg/µL for CBD. Transcript expression (**c**) in each treatment group was normalized to the GEOMEAN of 18 S and β-Actin, then compared to the gene in the control group, assessed using RT-qPCR. Significant differences were determined by a one-way ANOVA and corrected by a post-hoc Tukey test. Data presented as mean ± SEM ($n \geq 5$). Different letters denote significant differences of $p < 0.05$.

treatment, the cellular viability remained above 80%. Therefore, 10% CaSE was included in select functional assays to demonstrate the threshold of exposure-induced cytotoxic and metabolic responses but was omitted from molecular analyses (qPCR and Western blotting) due to limited cell viability. Further evaluations were carried out for markers of trophoblast fusion and differentiation using concentrations of 2.5% and 5% CaSE as well as 10 µM Δ9-THC; a concentration which we have previously shown to be non-cytotoxic in this cell line[22]. The impact of Δ9-THC and CaSE on trophoblast differentiation was assessed by quantifying the mRNA levels of human choriogonadotropin hormone (hCG), *CGα* (chorionic gonadotropin alpha), and *CGβ* (chorionic gonadotropin beta), as well as the total protein levels of hCG. Treatment with Δ9-THC exhibited a significant reduction in *CGβ* transcript levels ($p < 0.0001$), and no significant changes to hCG protein levels (Fig. 2a-c). However, 2.5% and 5.0% CaSE-treated cells showed a significant reduction in both *CGα* (Fig. 2a, $p < 0.0001$) and *CGβ* (Fig. 2b, $p < 0.0001$). In comparison to THC treatment, 2.5% and 5.0% CaSE treatments resulted in significant reductions in hCG protein content (Fig. 2c, $p < 0.05$). Given cell differentiation is inversely related to proliferative capacity, we assessed gene levels of a marker of cytotrophoblast proliferation, *KI67* (antigen Kiel 67), which was found to be decreased in the THC group (Fig. 2d, $p < 0.0001$) and increased in the 5.0% CaSE group (Fig. 2d, $p < 0.05$). As differentiation relies upon appropriate cell-cell fusion, we assessed cell fusion marker *ERVW-1* (endogenous retrovirus group W, member 1) and found mRNA levels decreased by treatments of THC (Fig. 2e, $p < 0.01$), and in both 2.5% and 5.0% CaSE-treated cells (Fig. 2d, $p < 0.001$).

Cannabis smoke exposure induces markers of cellular and oxidative stress, along with increased ROS levels

We investigated the cellular and mitochondrial stress related biochemical changes following cannabis smoke exposure by quantifying mRNA levels of *HSP60* (heat shock protein 60) and *HSP70* (heat shock protein 70), respectively. Cells treated with Δ9-THC for 48 h exhibited no changes in *HSP60*. In contrast, *HSP60* expression was significantly upregulated following 2.5% CaSE and 5.0% CaSE treatments (Fig. 3a, $p < 0.001$). Conversely, cells treated with THC and both 2.5% and 5.0% CaSE for 48 h exhibited a downregulation in *HSP70* mRNA levels (Fig. 3b, $p < 0.05$). Additionally, we assessed mRNA levels of antioxidant enzymes, superoxide dismutase 1 and 2, *SOD1* and *SOD2*. While transcript levels of *SOD1* were unchanged in Δ9-THC-treated cells, there was

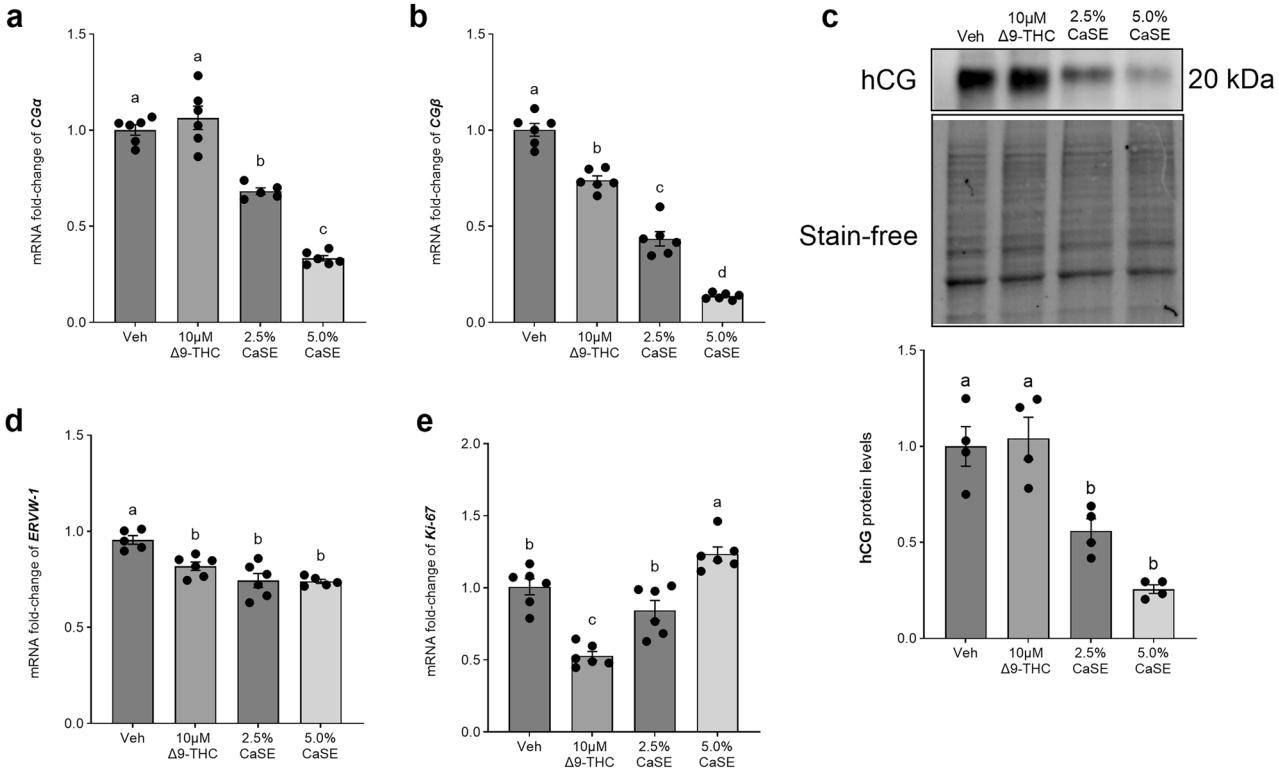

Fig. 2. CaSE impairs trophoblast fusion and differentiation. BeWo b30 cells were treated with vehicle (0.1% methanol), 10 µM THC, 2.5% or 5.0% CaSE for 48 h during differentiation. Transcript expression (**a**, **b**, **d**, **e**) in each treatment group was normalized to the GEOMEAN of 18 S and β-Actin. Cell lysates (25 µg/lane) were loaded and seperated on a 10% SDS-PAGE and the content of hCG was quantified using a rabbit polyclonal anti-hCG antibody. Summary histogram of relative protein levels of (**c**) hCG ($n = 4$) were assessed using Western blotting and normalized to the stain-free image. Cell lysates (25 µg/lane) were loaded on a 10% gel and SDS-PAGE and quantified using a rabbit polyclonal anti-hCG (DAKO, GA508) antibody. Significant differences were determined by a one-way ANOVA and corrected by a post-hoc Tukey test. Data presented as mean ± SEM ($n \geq 5$). Different letters denote significant differences of $p < 0.05$.

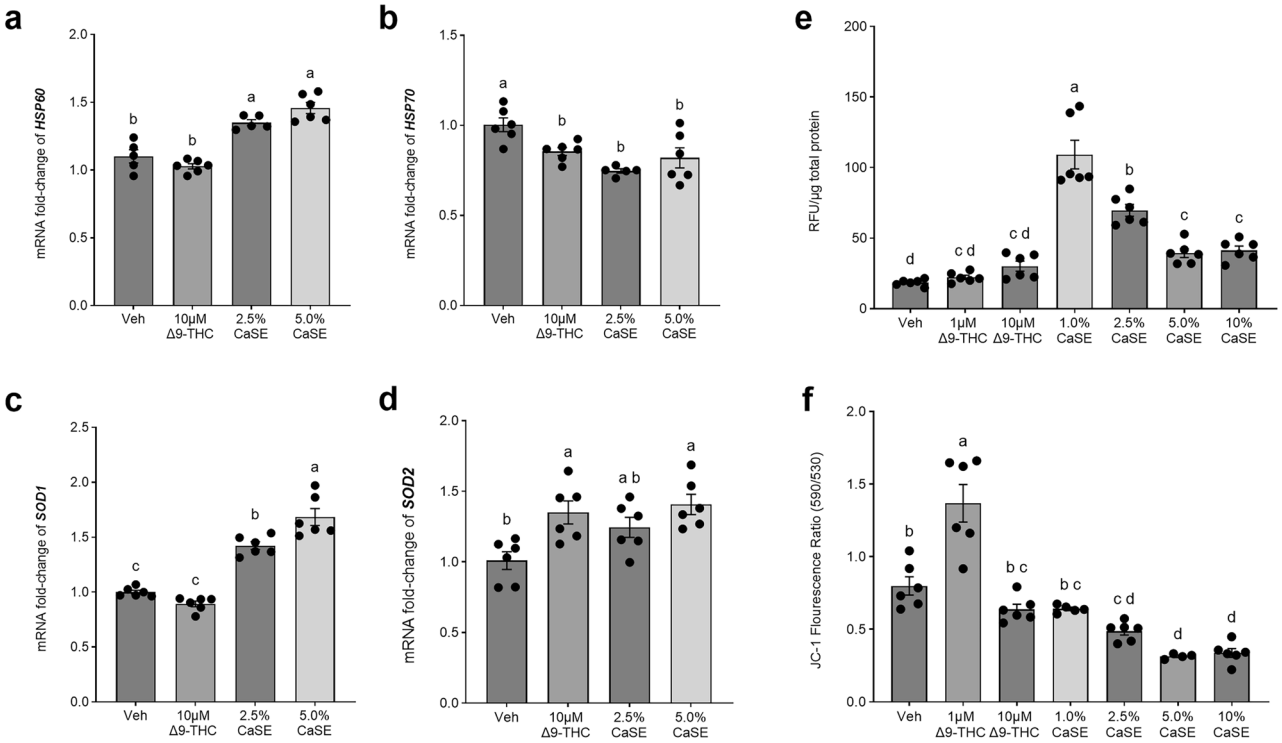

Fig. 3. CaSE induces ROS production and activates cellular and oxidative stress markers. BeWo b30 cells were treated with vehicle (0.1% methanol), 1 μM THC, 10 μM THC, and 1.0%, 2.5%, 5.0% or 10% CaSE for 48 h during differentiation. Transcript expression (**a**–**d**) in each treatment group was normalized to the GEOMEAN of 18 S and β-Actin, then compared to the gene in the control group, assessed using RT-qPCR. (**e**) The DCFDA assay was used to measure levels of reactive oxygen species; rotenone (10 nM) was used as a positive control. (**f**) The JC-1 assay was used to measure mitochondrial membrane potential (ΔΨm). Significant differences were determined by a one-way ANOVA and corrected by a post-hoc Tukey test. Data presented as mean ± SEM ($n \geq 5$). Different letters denote significant differences of $p < 0.05$.

an upregulation in 2.5% and 5.0% CaSE-treated cells (Fig. 3c, $p < 0.0001$). Furthermore, *SOD2* gene expression levels were increased in THC-treated cells (Fig. 3d, $p < 0.05$) and in 5.0% CaSE treated cells (Fig. 3d, $p < 0.01$). Due to the apparent alterations in superoxide dismutase expression, we quantified the intracellular levels of reactive oxygen species (ROS). We observed ROS levels were significantly increased with all CaSE treatments (Fig. 3e, $p < 0.001$); however, there were no substantial changes to ROS levels with Δ9-THC treatments. We then measured mitochondrial membrane potential using the JC-1 assay. Following treatment with 5.0% and 10% CaSE there was a reduction in membrane potential (Fig. 3f, $p < 0.05$) relative to the vehicle.

CaSE treatment results in attenuated basal respiration and ATP production

To establish the impacts of Δ9-THC and CaSE on parameters of mitochondrial respiration, we measured the oxygen consumption rate (OCR) using the Agilent Seahorse XF Mito Stress Test. We treated cells with a range of Δ9-THC and CaSE concentrations (1 μM, 10 μM, and 1%, 2.5%, 5%, 10%, respectively) for 48 h to establish dose-dependent relationships with drug exposure prior to the addition of oligomycin, FCCP (carbonyl cyanide-p-(trifluoromethoxy)phenylhydrazone) and antimycin A/rotenone. We found that 10 μM Δ9-THC and 5.0% CaSE decreased basal respiration (Fig. 4c, $p < 0.05$). Additionally, ATP production was also significantly reduced following 10 μM Δ9-THC and 5.0% CaSE (Fig. 4d, $p < 0.001$).We also observed proton leak, maximal respiratory capacity and non-mitochondrial respiration to be diminished with 5.0% and 10% CaSE (Supplementary Fig. S3).

The role of CB1 receptor-mediated signaling in facilitating the cellular effects of Δ9-THC and CaSE

To assess the impacts of CaSE and Δ9-THC on components of the endocannabinoid system (ECS), we assessed *CB1* (cannabinoid receptor 1) protein levels and found no significant changes with any treatment condition (Fig. 5a). To determine whether THC- and CaSE-driven changes to markers of syncytialization were mediated via the CB1 receptor, we pre-treated our cellswith 1 μM AM281 (CB1 antagonist) for 30 min followed by subsequent drug treatments with THC or CaSE for 48 h. We found that THC-induced changes to transcript levels of *CGB* and *ERVW-1* were rescued following CB1 receptor antagonism (Fig. 5e-f, $p < 0.05$). However, the effects on genes related to differentiation were not restored following CB1 receptor antagonism in CaSE-exposed cells. (Fig. 5e-f). Considering *CYP1A1* gene expression levels were stimulated following CaSE treatment, we evaluated the extent of AhR (aryl hydrocarbon receptor) stimulation. Gene expression levels of *AHR* were

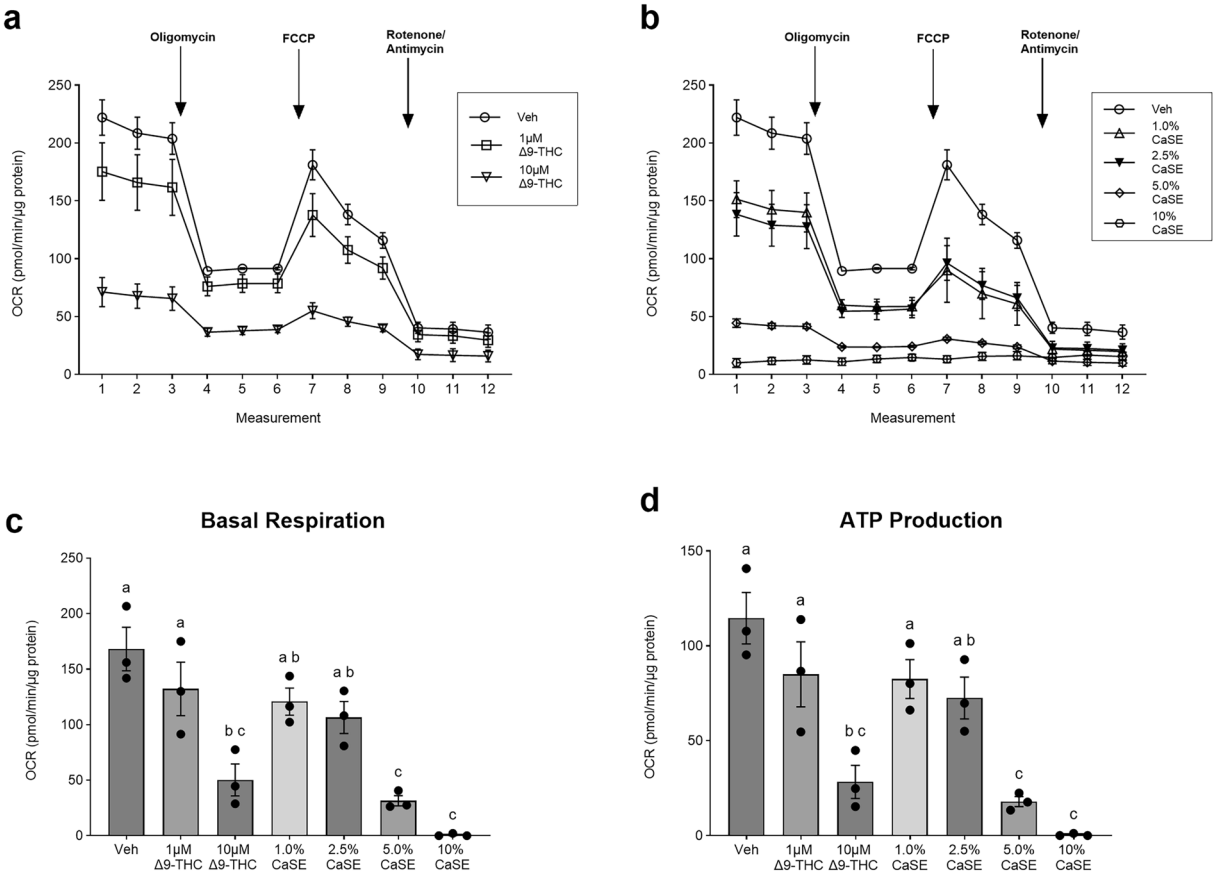

Fig. 4. High dose CaSE diminishes basal respiration rates and ATP production. BeWo b30 cells were treated with vehicle (0.1% methanol), 1 µM THC, 10 µM THC, 1%, 2.5%, 5.0% and 10% CaSE for 48 h during differentiation, and subjected to the mitochondrial stress test. Basal OCR tracings were obtained using the Seahorse XFe24 Analyzer using the sequential addition of oligomycin, FCCP and antimycin A/rotenone; values were normalized to total protein content via the BCA assay (µg/mL). The detection of OCR was performed with four technical replicates per experiment, for each treatment condition, and repeated three more times ($n = 3$ biological replicates). Group mean and SEM are displayed below (**a**-**d**). Arrows indicate the sequential addition of the respective compounds. Significant differences were determined by a one-way ANOVA and corrected by a post-hoc Tukey test. Different letters denote significant differences of $p < 0.05$. (**a**, **b**) Oxygen consumption rate (OCR) tracings, (**c**) Basal respiration, (**d**) ATP-linked Production.

unchanged following Δ9-THC treatment and CaSE exposure (Fig. 5b). However, transcript levels of *AHRR* (aryl hydrocarbon receptor repressor) were upregulated with 2.5% CaSE treatment (Fig. 5c, $p < 0.0001$).

Discussion

To our knowledge, this study is the first to examine the effects of cannabis smoke extract (CaSE) on human placental trophoblast cells. Cannabis smoke represents a complex mixture resulting from the pyrolysis of the plant, containing numerous combustion products such as PAHs, nitric oxide, carbon monoxide, and aryl amines[12]. While Δ9-THC and CBD are the most abundant bioactive compounds found in commercially available cannabis products, studying these cannabinoids in isolation may overlook the complex pharmacological and toxicological properties within whole cannabis smoke[26]. Indeed, results from this study have identified differences in the effects of THC alone and CaSE on trophoblast cell differentiation and mitochondrial function, which is summarized in Table S2.

We found that Δ9-THC concentrations in our 2.5% and 5.0% CaSE were ~ 1.74 (± 0.18) µM (~ 547.23 ng/mL) and 4.30 (± 0.18) µM (~ 1352.4 ng/mL), respectively, generated from a 12–14% THC-dominant cannabis cigarette (Fig. 1a). Such levels are comparable to those found in cannabis smokers and in human placental tissue (100–432 ng/g), although some of these findings are derived from cannabis cigarettes with lower THC percentages[27,28]. AhR is primarily activated following exposure to PAHs, such as benzopyrene and benzanthracene, as well aryl-containing amines[29], which leads to the induction of its downstream target CYP1A1 – a phase I drug metabolizing enzyme. This enzyme is expressed by placental tissue and is important in metabolizing xenobiotic compounds, including environmental toxicants[30]. While some studies have demonstrated Δ^9-THC itself can inhibit CYP1A1 activity and partially activate its expression through the AhR[29], we did not find any significant induction of CYP1A1 expression. Conversely, CaSE treatment resulted in a profound increase in the expression of CYP1A1

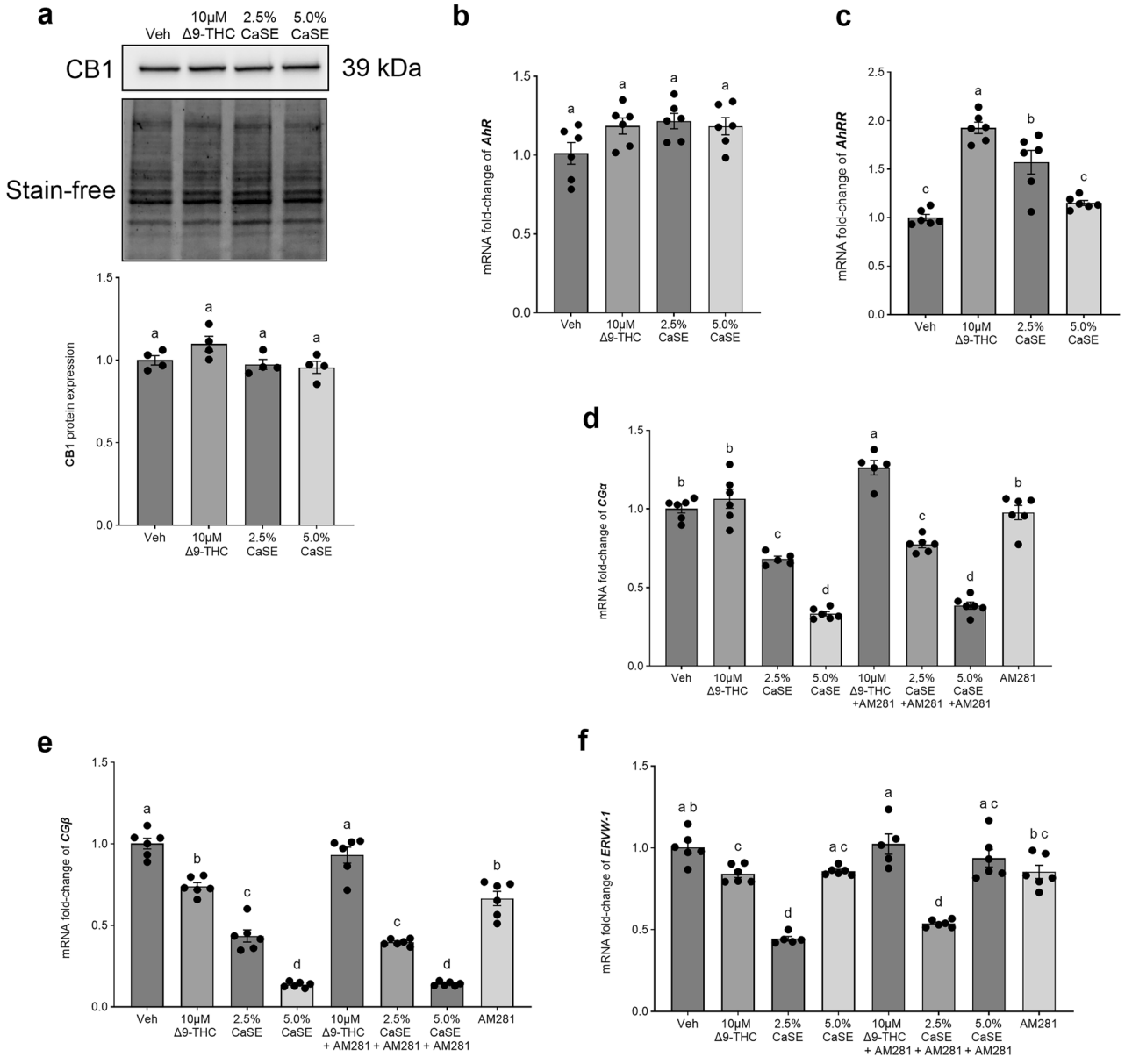

Fig. 5. CB1R antagonist treatment does not restore CaSE-induced disruptions to differentiation markers. BeWo b30 cells were treated with vehicle (0.1% methanol), 10 μM THC, 2.5% and 5.0% CaSE for 48 h during differentiation, and a subset of cells were pre-treated with AM281 (1 μM) for 30 min and then treated with the corresponding treatment. Summary histogram displaying the relative changes in protein levels of (**a**) CB1 ($n = 4$) were assessed using Western blotting and normalized to the stain-free image. Cell lysates (25 μg/lane) were loaded and seperated on a 4–20% SDS-PAGE and quantified using a rabbit polyclonal anti-CB1 antibody. Transcript expression (**b**–**f**) in each treatment group was normalized to the GEOMEAN of 18 S and β-Actin, then compared to the gene in the control group, assessed using RT-qPCR. Significant differences were determined by a one-way ANOVA and corrected by a post-hoc Tukey test. Data presented as mean ± SEM ($n \geq 5$). Different letters denote significant differences of $p < 0.05$.

transcript levels (Fig. 1c), likely due to the presence of AhR-activating ligands in CaSE. These findings point to the complex mixture effects that result from combustion-derived constituents in cannabis smoke in tandem with the phytocannabinoids. Thus, conclusions drawn from studies using single cannabinoids may overlook critical aspects of xenobiotic metabolism, toxicity and cellular damage associated with cannabis smoke exposure.

Cytotrophoblasts differentiate into a syncytium that plays a critical role in producing and releasing hormones important for initiating, regulating and maintaining pregnancy, an example of which is human chorionic gonadotropin (hCG)[31]. This hormone consists of two subunits, alpha (CGα) and beta (CGb)[32,33]. It has been widely recognized, both in vitro and in vivo, that PAH exposure and tobacco smoking are correlated with reduced hCG levels[33,34]. Despite the conflicting evidence in the literature as to whether cannabis directly impacts serum hCG levels, confirmed pregnant cannabis smokers have shown higher rates of pregnancy loss compared to non-

smokers, which may be due, in part, to cannabinoid-induced reductions in hCG levels[35,36]. Here, we report a dose-dependent reduction of both hCG transcript and protein expression (Fig. 2a) following exposure to CaSE, however treatment with THC alone only caused a significant reduction in CGb expression and not hCG protein. Previous work by our group has shown that despite reduced cell-cell fusion with 10 μM Δ9-THC, only higher THC doses impaired hCG secretion[22]. Moreover, we observed that transcript levels of *ERVW-1* were reduced with both CaSE and 10 μM Δ9-THC treatment. Taken together these data suggest that THC plays a critical role in the differentiation of CTs into the multinucleated syncytiotrophoblast. To understand the differences between THC and CaSE exposure we also measured expression of a proliferative marker, Ki67. CaSE significantly upregulated and THC significantly downregulated the expression of *Ki67* (Fig. 2e). During syncytialization, the proliferative capacity of STs is dramatically reduced as differentiation progresses into mitotically inactive cells[37]. Our results suggest constituents within cannabis smoke may impair differentiation by sustaining a proliferative state, disrupting the transition from CTs into terminally differentiated STs. In fact, with our CaSE treatment, lower concentrations of Δ9-THC (~ 4.30 μM) within the smoke matrix are more damaging to syncytialization compared to single component THC treatment.

Proper syncytium formation requires the coordinated balance of oxidative stress pathways that underpin placental development[38]. We assessed mitochondrial function to investigate whether cannabis related disruptions to metabolic homeostasis could be contributing to impaired trophoblast differentiation. Previous work from our group has linked impaired mitochondrial respiration and redox signaling to disruptions in trophoblast fusion and hormone production in trophoblast cells[39]. Mitochondrial dysfunction in the placenta, characterized by oxidative stress and disrupted cellular bioenergetics, has been implicated in poor pregnancy outcomes (e.g. IUGR)[40,41], which are consequences that have been associated with prenatal cannabis use[42]. Oxidative stress occurs from the imbalance of the oxidant and antioxidant systems – this can arise from the excessive production of pro-oxidants and/or the inability of antioxidants to mitigate pro-oxidants[43]. Cannabis smoke, like cigarette smoke, contains a myriad of pro-oxidants, namely superoxide radicals, nitric oxide and other unstable free radicals[44]. Additionally, endogenous sources of pro-oxidants, including derivatives of molecular oxygen (O_2) like superoxide ($O_2^{\bullet -}$) and hydrogen peroxides (H_2O_2) produced by the mitochondrial electron transport chain (ETC) can contribute to oxidative stress following smoke exposure[45,46]. In our study, CaSE significantly increased intracellular ROS levels at low dose CaSE (1% and 2.5%), but ROS levels began to decline at higher doses (5% and 10% CaSE). Mitochondrial membrane potential was preserved at low CaSE doses but decreased at high doses (Fig. 3f). Our dose-dependent changes to ROS and membrane potential may indicate early oxidative stress likely driven by combustion-derived exogenous radicals. Indeed, Sarafian et al. demonstrated in vitro exposure to cannabis smoke, but not Δ9-THC, significantly increased ROS levels, suggesting that pyrolytic byproducts from the smoke may act independently or synergize with cannabinoids to drive ROS production[47].

To determine whether the antioxidant defense system may have been primed to respond to this oxidative burden, we evaluated two key antioxidant markers, SOD1 and SOD2, which localize to the cytoplasmic and mitochondrial compartments of the cell, respectively[48]. Consistent with our observations of differential ROS production at low or high doses of CaSE, we found only *SOD1* to be induced with lower CaSE, whereas higher doses of CaSE were associated with upregulations of both *SOD1* and *SOD2* (Fig. 3c-d). Interestingly, THC alone induced *SOD2*, indicating a mitochondrial targeted response. Mitochondrial and cytosolic stress markers, *HSP60* and *HSP70*, were differentially regulated (Fig. 3A and B), pointing to the differential intracellular stress pathways that are activated with CaSE versus Δ9-THC. Raja et al. demonstrated the differences to antioxidant stimulation in neuronal SY-SH5Y cells and attributed this to varying THC/CBD ratios present in cannabis extracts[49]. Importantly, our differences may indeed relate to the inherent antioxidant properties of phytocannabinoids, which are modulated or overlooked in the context of smoke exposure. At higher CaSE concentrations (5% and 10%), decreased ROS production was observed concomitantly with reduced mitochondrial membrane potential, as well as diminished basal respiration rates and ATP production, suggesting ETC dysfunction (Figs. 3f and 4a-b). This is consistent with work showing that both cannabis smoke and Δ9-THC impair mitochondrial function and reduce ATP production in vitro[47,50,51]. Taken together, these data imply a biphasic metabolic reprogramming and stress response, wherein low dose CaSE induces mitochondrial respiration impairment, accompanied with increasing ROS from ETC derived electron leakage, and corresponding activation of antioxidant defenses. Contrastingly, the higher dose CaSE causes more severe ETC impairment, leading to reduced ROS production resulting from the minimal electron flow and reduced membrane potential. Previous work from our lab has shown cannabinoids (D9-THC and CBD) alter cellular bioenergetics, with the greatest impairments observed at higher D9-THC dosages (10 μM-20 μM) relative to lower D9-THC dosages (1 μM)[22,23], which supports the notion that exposure to elevated concentrations of THC induces greater ROS production and attenuation of ATP production, compared to lower doses of D9-THC. Interestingly, this dose-dependent relationship in the present study revealed that lower effective concentrations of D9-THC within CaSE (4.3 μM D9-THC in 5.0% CaSE) elicited equal impairments in mitochondrial respiration compared to single component D9-THC (10 μM) exposure (Fig. 4a-b). These effects were accompanied by alterations in additional Seahorse parameters including increased proton leak and changes in non-mitochondrial respiration, further supporting CaSE-induced disruption of mitochondrial function (Supplemental Fig. S3(a-c)). These results highlight the importance of considering complex smoke mixtures versus isolated cannabinoids when evaluating cellular bioenergetics and trophoblast health. It is also worth noting that impairments in mitochondrial function can impact cellular glucose levels. Although glucose metabolism was not directly explored in this study, future investigations comparing the effects of CaSE and individual cannabinoids on trophoblast glucose metabolism and glycolytic flux could provide valuable insights into these metabolic adaptations. More broadly, our findings that smoke extract-disrupted mitochondrial bioenergetics observed during trophoblast differentiation may have important implications for proper placental development and efficiency[39].

Cannabinoid receptor signaling is instrumental during pregnancy and therefore warrants careful consideration in the context of prenatal cannabinoid exposures[52]. For the purposes of this study, we focused on CB1 receptor pharmacology as a proxy to reveal the complex ECS receptor changes induced by Δ9-THC and smoke exposure. CB1 is one of the most well-known receptors in the ECS and has a widely recognized role in trophoblast differentiation and overall reproductive success[52–55]. Δ9-THC and its corresponding metabolite, 11-hydroxy-THC, are partial agonists of the CB1 receptor, making this a relevant target in the context of cannabis extract exposure[56]. We report that protein levels of CB1R do not change following treatment with either Δ9-THC treatment or smoke extract (Fig. 5a). Chronic cannabis use has been shown to desensitize the CB1 receptor, without reducing receptor protein levels, which is consistent with our findings[57]. Our observation that 10 μM Δ9-THC does not alter CB1 receptor protein expression is also consistent with reports following both 24 h and 72 h exposure in placental explants[58]. In our study, incubation with a CB1 receptor antagonist revealed that Δ9-THC impacted trophoblast differentiation through CB1 receptor-mediated signaling (Fig. 5d-f) an effect which is consistent with previous work from our group[22]. In the presence of the CB1-receptor antagonist AM281 with CaSE, there was neither blockage nor attenuation of any adverse effects related to reduced differentiation markers induced by the CaSE treatment (Fig. 5d-f). Therefore, the exposure to AhR ligands generated by the CaSE treatment may point to potential pathways that smoke may be acting through to cause the adverse effects related to differentiation[59].

While this study provides novel insights into cannabis smoke-induced dysfunction in trophoblasts, there are some limitations to consider. BeWo b30 cells are a third-trimester choriocarcinoma cell line that resembles cytotrophoblast-like cells capable of differentiating into syncytiotrophoblast, which are cell populations that reside at the maternal-fetal interface. The differentiation of cytotrophoblasts into syncytiotrophoblast is a process that occurs continuously throughout gestation, underscoring the relevance of this model in capturing the dynamic nature of placental biology[60,61]. We modeled this differentiation process over a 48-hour period, as this timeframe is commonly used to capture syncytialization in vitro[61]. This approach allowed us to assess the direct cellular effects of combustion-derived constituents and cannabinoids on trophoblast physiology during differentiation in a controlled environment. Our 48-hour treatment window represents an acute exposure at the cellular level rather than a chronic in vitro exposure, providing insight into the immediate effects of cannabis smoke extract on trophoblast function. Future studies could expand upon these findings by investigating both short- and long-term exposures to model acute versus chronic cannabis smokeexposure. Additionally, examining the baseline effects of CaSE and D9-THC on undifferentiated cytotrophoblast cells prior to syncytialization would help delineate initial cellular changes that precede the differentiation-associated responses.

In the present study, we showed cannabis smoke extract differentially alters key pathways involved in trophoblast metabolism and differentiation. Our work offers insights into the complexity of cannabis smoke versus treatments with synthetic cannabinoids such as Δ9-THC, and underscores the importance of including combustion-derived constituents in reproductive smoking models. Taken together, our findings demonstrate the urgent need to evaluate cannabis smoke as a toxicological exposure route in reproductive health. It also provides valuable insights for understanding the mechanistic underpinnings of cannabis smoke-induced dysfunction in trophoblast cells and develop harm reduction strategies for prenatal cannabis use. Future studies should consider cannabinoid profiles that mirror the evolving cannabis market as well as routes of exposure such as smoking, which persists as the primary route of self-administering cannabis during pregnancy[1].

Methods

Cell culture

BeWo b30 cells (AddexBio, C0030002) were cultured in in 1X Dulbecco's Modified Eagle Medium (1X DMEM) containing 4.5 g/L glucose, L-glutamine, sodium pyruvate supplemented with 10% heat-inactivated fetal bovine serum (HI-FBS), 1% penicillin-streptomycin and 1% L-glutamine, incubated at 37 °C and 5% CO_2 conditions. Cells were plated on multi-well plates at a seeding density of approximately 1×10^5 cells/cm^2 to achieve ~90% confluency. Following 24 h of cell adherence, epidermal growth factor (EGF; 50 ng/mL) was added to the media to stimulate monolayer formation and proliferation. After 48 h, cells were treated with forskolin-1 (FSK; 50 μM) along with additional EGF to induce trophoblast differentiation and fusion of syncytiotrophoblast (ST) for a 48-hour duration. At the time of FSK and EGF addition, cells were treated with either vehicle control (0.1% methanol), 1 μM or 10 μM Δ9-THC, or 1.0%, 2.5%, 5.0% or 10% cannabis smoke extract (CaSE). Smoke-treated cultured cells were kept in a separate incubator at 37 °C and 5% CO_2 conditions for the duration of the exposure.

Preparation of cannabis smoke extract

THC-dominant, dried cannabis flower was purchased from Cannalogue Labs (14% THC: 1% CBD). Cigarettes were hand-packed into king size cigarette tubes, each containing ~0.70 g of dried cannabis. Prior to use, the filter of each cigarette was removed. Briefly, CaSE was prepared by drawing smoke, under vacuum, through 10 mL of cell culture media. On average, the burn duration for each cigarette was 2:30 min. The CaSE was then passed through a 0.22 μm filter and diluted either 1:100 (1%), 1:40 (2.5%), 1:20 (5%), or 1:10 (10%), using fresh cell culture media (described above). Fixed combustion times, burn rates, and day-of-use were parameters consistently and carefully considered to ensure reproducibility.

Detection and Quantitation of Cannabinoids by LC-MS/MS

Smoke extract media (before and after filtration) and sample supernatants were analyzed using targeted liquid chromatography–tandem mass spectrometry (LC–MS/MS) for the quantification of phytocannabinoids (THC and CBD). Native and isotopically labeled standards (d_3-THC and d_3-CBD; purity > 98%) were obtained from Toronto Research Chemicals and stored at 4 °C.

Method performance was evaluated by spiking in vitro media (60 µL) with THC and CBD at three concentrations (10, 500, and 1500 pg/µL; $n = 6$ for each level), followed by dilution to 1500 µL with acetonitrile. Across all spike levels, analyte recoveries exceeded 90% and repeatability was better than 15%. Limits of detection (LODs) were determined in accordance with the Eurachem Guide to Method Validation using the equation:

$$\mathrm{LOD} = 3 \times s'_o \times \sqrt{1/n}$$

where $s'_o$is the adjusted standard deviation calculated from replicate measurements of media spiked at 10 pg/µL[63]. Resulting LODs were 7.5 pg/µL for THC and 7.1 pg/µL for CBD. Limits of quantitation (LOQs) were determined by substituting 10 for the factor of 3 in the equation above: yielding LOQs of 25.3 pg/ µL for THC and 23.5 pg/µL for CBD. For sample quantification, 60 µL of in vitro media was transferred to an LC vial, fortified with 20 µL of d_3-THC and d_3-CBD internal standards (7.5 ng/µL), and diluted to a final volume of 1500 µL with acetonitrile. Chromatographic separation was performed on an XSelect HSS T3 C18 column (2.5 µm, 2.1 mm × 50 mm) using a binary mobile phase consisting of methanol and water. Mass spectrometric detection was carried out using positive electrospray ionization on an AB Sciex 365 triple quadrupole instrument equipped with an HSID Ionics Eclipse 10 Plus orthogonal ionization source. Additional details, including the HPLC gradient and multiple reaction monitoring ion transitions used for THC and CBD quantification, are provided in Brown et al. (2019)[58].

Cell viability

Cells were seeded and treated in 96-well plates with varying dilutions of CaSE as described above. Following treatment, 10% AlamarBlue (Bio-Rad Laboratories) was added to fresh media, and cells were incubated at 37 °C in 5% CO_2 for 4 h, protected from light. Absorbance was read at 570 nm and 600 nm for test and blank wells, respectively, in a microplate reader (Tecan Spark® Multimode Microplate Reader).

RNA extraction & real-time quantitative PCR

Total RNA was isolated from BeWo b30 cells grown, treated, and harvested from 6-well plates as previously described. Briefly, cells were lysed with 500 µl of ice-cold TRIzol ™ reagent (Thermo Fisher Scientific) and total RNA, was extracted using the Direct-zol RNA MiniPrep Kit (Zymo Research) according to the manufacturers protocol. ~1 µg of RNA was converted to complementary DNA (cDNA) using the High-Capacity cDNA Reverse Transcription Kit (Applied Biosystems™) as per the manufacturer instructions. Quantitative real-time PCR was used to measure mRNA expression detected with GB-Amp™ SYBR Green qPCR Mix (GeneBio Systems) using the CFX384 Touch ™ Real-Time PCR Detection System (Bio-Rad Laboratories) Analysis of fold-change in mRNA expression levels was calculated using the double-delta ($2^{-\Delta\Delta CT}$) method, normalized to the geometric means of reference gene expression levels (18 S, β-Actin) and then to the vehicle control. Primer sequences can be found in Supplementary Table S1.

BCA (Bicinchoninic Assay)

Protein concentration of samples was determined using the bicinchoninic assay (BCA; ThermoFisher). Total protein concentration was measured at an absorbance of 562 nm in a 96-well plate using a microplate reader (Tecan Spark® Multimode Microplate Reader).

SDS-PAGE and Western blotting

Cells treated with Δ9-THC and CaSE were harvested using radioimmunoprecipitation assay (RIPA) lysis buffer, containing phosphatase and protease inhibitors (Roche Diagnostics). Samples were prepared from total protein extract, Laemelli Sample Buffer (2X) and β-mercaptoethanol. Proteins (20–25 µg/sample) were separated by gel electrophoresis using Mini-PROTEAN® TGX Stain-Free™ gels. Following electrophoretic separation, the gels (Bio-Rad Laboratories) were transferred onto PVDF membranes using the Trans-Blot® Turbo™ Transfer System (Bio-Rad Laboratories). Membranes were blocked in 1X Tris-buffered saline-Tween 20 buffer with 5% BSA and probed using anti-hCG (DAKO; Cat. #: GA508; Lot #: 20016637; rabbit polyclonal; 1:1000) and anti-CB1R (Cayman; Cat. #: 10006590; Lot #: 0577427-1; rabbit polyclonal, 1:5000) in the blocking solution. Donkey anti-rabbit (1:10,000) secondary antibodies were used for immunodetection of the primary antibody. Proteins were visualized using Clarity Max Western ECL Substrate (Bio-Rad Laboratories) and visualized using ChemiDoc Imaging System (Bio-Rad Laboratories). Band intensities were quantified using Image Lab (Bio-Rad Laboratories). Proteins of interest were normalized to total protein content on the corresponding membrane following visualization with stain-free imaging technology.

DCFDA assay (2′,7′-dichlorofloroescin diacetate)

Reactive oxygen species (ROS) were detected using the DCFDA/ H2DCFDA Cellular ROS Detection Assay Kit (Abcam, ab113851) as per the manufacturer's instructions. Briefly, cells were seeded in a black, clear bottom 96-well microplate at a cell density of 32,000 cells; differentiated and treated as described above. Following 48 h of treatment, media was removed, and the cells were washed with 1X Buffer (90% ddH_2O, 10% 10X Buffer), then incubated with DCFDA (5 µM) for 45 min. The resulting fluorescent signal wasquantified at an excitation/ emission of 485/535nm (Tecan Spark® Multimode Microplate Reader). All readings were normalized to total protein content via the BCA assay.

Mitochondrial respiration assay

The mitochondrial oxygen consumption rate (OCR) was measured at 37 °C in an XFe24 Extracellular Flux Analyzer (Agilent Bioscience). BeWo b30 cells were seeded at 50,000 cells/well in 250 µl culture media in 24-well

microplates; and were differentiated and treated as described above. Following 48 h, cultured media was removed and replaced with XF base medium (Seahorse Bioscience) supplemented with 100 mM sodium pyruvate, 200 mM L-glutamine, and 5 mL of 45% glucose solution, warmed to 37 °C (pH 7.4). The assay medium was then pre-equilibrated to 37 °C for 1 h. The OCR was detected under basal conditions followed by the sequential injection of oligomycin (ATP synthase inhibitor), carbonyl cyanide-4- (trifluoromethoxy)phenylhydrazone (FCCP; mitochondrial uncoupler) and rotenone combined with antimycin A (complex I and III electron transport blockers) through ports of the Seahorse Flux Pak cartridges to achieve final concentrations of 1, 0.3 and 0.5 µM, respectively. OCR values were normalized to total protein content from each well determined through the BCA assay. Each OCR detection experiment was performed with four technical replicates per experiment, for each treatment condition, to obtain an average response per experiment. Each experiment was repeated 3 times.

Mitochondrial membrane potential

Mitochondrial membrane potential (ΔΨm) was assessed using the fluorescent reagent tetraethylbenzimidazolylcarbocyanine iodide (JC-1) with the JC-1-Mitochondrial Membrane Potential Assay kit (Abcam, ab113850) following the manufacturer's instructions. Briefly, cells were seeded in a black, clear bottom 96-well microplates at a cell density of 32,000 cells, differentiated and treated as described above. Following 48 h, cells were washed once with 1X dilution buffer (90% ddH_2O, 10% 10X Dilution Buffer) and incubated with the JC-1 dye (20 µM) in 1X dilution buffer for 10 min at 37 °C, protected from light. The dye was then removed, cells were washed once with 1X dilution buffer and 100 µl of 1X Supplemented Buffer (2% FBS, 98% ddH_2O) was added. The red fluorescence intensity (excitation/emission (535 nm/590 nm)) and green fluorescence (excitation/emission (475 nm/530 nm)) were measured using a microplate reader (Tecan Spark® Multimode Microplate Reader). Background fluorescence was subtracted, and the ratio of red (polarized) fluorescence divided by green (depolarized) fluorescence was calculated.

Evaluation of antagonism at CB1 receptor(s)

The efficacy of Δ9-THC and CaSE at CB1 receptors on BeWo b30 cells was evaluated by pre-incubating with a selective CB1 antagonist, AM281 (1 µM) for 30 min prior to drug treatments. The concentration and incubation period were selected based on previous studies demonstrating effective CB1R blocking at 1 µM[22,64,65]. Following the pre-incubation, a subset of cells was re-incubated with the AM281 and corresponding treatment; cells were treated and differentiated as described above.

Statistical analyses

All statistical analyses were performed using GraphPad Prism software V6.0. All experiments were performed with six biological replicates (unless otherwise specified). All outliers were identified with a Grubbs' test (alpha = 0.05) followed by an assessment for normal distribution using the Shapiro-Wilk test. A one-way ANOVA (analysis of variance) was used to compare differences among two or more groups, followed by a post-hoc Tukey test for multiple comparisons. Data is reported as means ± S.E.M., unless otherwise stated. Different letters denote significant differences, which is defined as a statistical threshold of $p < 0.05$.

Data availability

All data presented in the article and supplementary information files can be obtained from the corresponding author upon request.

Received: 5 September 2025; Accepted: 18 January 2026
Published online: 26 January 2026

References

1. Young-Wolff, K. C. et al. Sociodemographic differences in modes of cannabis use among pregnant individuals in Northern California. *Drug Alcohol Depend.* **267**, 112546. https://doi.org/10.1016/j.drugalcdep.2024.112546 (2025).
2. Brik, M. et al. Cannabis exposure during pregnancy and perinatal outcomes: A cohort study. *Acta Obstet. Gynecol. Scand.* **103**, 1083–1091. https://doi.org/10.1111/aogs.14818 (2024).
3. Varner, M. W. et al. Association between stillbirth and illicit drug use and smoking during pregnancy. *Obstet. Gynecol.* **123**, 113–125. https://doi.org/10.1097/AOG.0000000000000052 (2014).
4. Holme, J. A. et al. Polycyclic aromatic hydrocarbons (PAHs) May explain the Paradoxical effects of cigarette use on preeclampsia (PE). *Toxicology* **473**, 153206. https://doi.org/10.1016/j.tox.2022.153206 (2022).
5. Natale, B. V. et al. Δ9-tetrahydrocannabinol exposure during rat pregnancy leads to symmetrical fetal growth restriction and labyrinth-specific vascular defects in the placenta. *Sci. Rep.* **10**, 544. https://doi.org/10.1038/s41598-019-57318-6 (2020).
6. Allen, S. et al. Cannabidiol exposure during rat pregnancy leads to Labyrinth-Specific vascular defects in the placenta and reduced fetal growth. *Cannabis Cannabinoid Res.* **9**, 766–780. https://doi.org/10.1089/can.2023.0166 (2024).
7. Weyrich, L. et al. Altered functional connectivity and oscillatory dynamics in polysubstance and cannabis only users during visuospatial processing. *Psychopharmacol. (Berl).* **240**, 769–783. https://doi.org/10.1007/s00213-023-06318-6 (2023).
8. Gunn, J. K. et al. Prenatal exposure to cannabis and maternal and child health outcomes: a systematic review and meta-analysis. *BMJ Open.* **6**, e009986. https://doi.org/10.1136/bmjopen-2015-009986 (2016).
9. Conner, S. N. et al. Maternal marijuana use and adverse neonatal outcomes: A systematic review and Meta-analysis. *Obstet. Gynecol.* **128**, 713–723. https://doi.org/10.1097/AOG.0000000000001649 (2016).
10. Wishart, D. S. et al. Correction to chemical composition of commercial cannabis. *J. Agric. Food Chem.* **72**, 14479. https://doi.org/10.1021/acs.jafc.4c01418 (2024).
11. Rock, E. M. & Parker, L. A. Constituents of cannabis sativa. *Adv. Exp. Med. Biol.* **1264**, 1–13. https://doi.org/10.1007/978-3-030-57369-0_1 (2021).
12. Graves, B. M. et al. Comprehensive characterization of mainstream marijuana and tobacco smoke. *Sci. Rep.* **10**, 7160. https://doi.org/10.1038/s41598-020-63120-6 (2020).
13. Ellis, R. J. et al. Prenatal Δ. *Biol. Psychiatry*. **92**, 127–138. https://doi.org/10.1016/j.biopsych.2021.09.017 (2022).

14. de Salas-Quiroga, A. et al. Prenatal exposure to cannabinoids evokes long-lasting functional alterations by targeting CB1 receptors on developing cortical neurons. *Proc. Natl. Acad. Sci. U S A.* **112**, 13693–13698. https://doi.org/10.1073/pnas.1514962112 (2015).
15. Lee, K. et al. Cannabidiol exposure during gestation leads to adverse cardiac outcomes early in postnatal life in male rat offspring. *Cannabis Cannabinoid Res.* https://doi.org/10.1089/can.2023.0213 (2024).
16. Vargish, G. A. et al. Persistent inhibitory circuit defects and disrupted social behaviour following in utero exogenous cannabinoid exposure. *Mol. Psychiatry*. **22**, 56–67. https://doi.org/10.1038/mp.2016.17 (2017).
17. Ferber, S. G. et al. The entourage effect: terpenes coupled with cannabinoids for the treatment of mood disorders and anxiety disorders. *Curr. Neuropharmacol.* **18**, 87–96. https://doi.org/10.2174/1570159X17666190903103923 (2020).
18. Metz, T. D. et al. Cannabis exposure and adverse pregnancy outcomes related to placental function. *JAMA* **330**, 2191–2199. https://doi.org/10.1001/jama.2023.21146 (2023).
19. O'Brien, K., Wang, Y. & The Placenta A maternofetal interface. *Annu. Rev. Nutr.* **43**, 301–325. https://doi.org/10.1146/annurev-nutr-061121-085246 (2023).
20. Turco, M. Y. & Moffett, A. Development of the human placenta. *Development* **146** https://doi.org/10.1242/dev.163428 (2019).
21. Lu, M. & Sferruzzi-Perri, A. N. Placental mitochondrial function in response to gestational exposures. *Placenta* **104**, 124–137. https://doi.org/10.1016/j.placenta.2020.11.012 (2021).
22. Walker, O. S. et al. Delta-9-tetrahydrocannabinol disrupts mitochondrial function and attenuates syncytialization in human placental bewo cells. *Physiol. Rep.* **8**, e14476. https://doi.org/10.14814/phy2.14476 (2020).
23. Podinic, T. et al. Cannabidiol disrupts mitochondrial respiration and metabolism and dysregulates trophoblast cell differentiation. *Cells* **13** https://doi.org/10.3390/cells13060486 (2024).
24. Black, T. et al. Differential effects of gestational cannabis smoke and phytocannabinoid injections on male and female rat offspring behavior. *Prog Neuropsychopharmacol. Biol. Psychiatry*. **136**, 111241. https://doi.org/10.1016/j.pnpbp.2024.111241 (2025).
25. Black, T. et al. Characterization of cannabinoid plasma concentration, maternal health, and cytokine levels in a rat model of prenatal cannabis smoke exposure. *Sci. Rep.* **13**, 21070. https://doi.org/10.1038/s41598-023-47861-8 (2023).
26. Sharma, P., Murthy, P. & Bharath, M. M. Chemistry, metabolism, and toxicology of cannabis: clinical implications. *Iran. J. Psychiatry*. **7**, 149–156 (2012).
27. Falcon, M. et al. Maternal hair testing for the assessment of fetal exposure to drug of abuse during early pregnancy: comparison with testing in placental and fetal remains. *Forensic Sci. Int.* **218**, 92–96. https://doi.org/10.1016/j.forsciint.2011.10.022 (2012).
28. Schwope, D. M., Karschner, E. L., Gorelick, D. A. & Huestis, M. A. Identification of recent cannabis use: whole-blood and plasma free and glucuronidated cannabinoid pharmacokinetics following controlled smoked cannabis administration. *Clin. Chem.* **57**, 1406–1414. https://doi.org/10.1373/clinchem.2011.171777 (2011).
29. Roth, M. D. et al. Induction and regulation of the carcinogen-metabolizing enzyme CYP1A1 by marijuana smoke and delta (9)-tetrahydrocannabinol. *Am. J. Respir. Cell Mol. Biol.* **24**, 339–344. https://doi.org/10.1165/ajrcmb.24.3.4252 (2001).
30. Stejskalova, L. & Pavek, P. The function of cytochrome P450 1A1 enzyme (CYP1A1) and Aryl hydrocarbon receptor (AhR) in the placenta. *Curr. Pharm. Biotechnol.* **12**, 715–730. https://doi.org/10.2174/138920111795470994 (2011).
31. Cole, L. A. Biological functions of hCG and hCG-related molecules. *Reprod. Biol. Endocrinol.* **8**, 102. https://doi.org/10.1186/1477-7827-8-102 (2010).
32. Stenman, U. H., Tiitinen, A., Alfthan, H. & Valmu, L. The classification, functions and clinical use of different isoforms of HCG. *Hum. Reprod. Update*. **12**, 769–784. https://doi.org/10.1093/humupd/dml029 (2006).
33. Drwal, E., Rak, A., Tworzydło, W. & Gregoraszczuk, E. Real life polycyclic aromatic hydrocarbon (PAH) mixtures modulate hCG, hPL and hPLGF levels and disrupt the physiological ratio of MMP-2 to MMP-9 and VEGF expression in human placenta cell lines. *Reprod. Toxicol.* **95**, 1–10.https://doi.org/10.1016/j.reprotox.2020.02.006 (2020).
34. Bernstein, L. et al. Cigarette smoking in pregnancy results in marked decrease in maternal hCG and oestradiol levels. *Br. J. Obstet. Gynaecol.* **96**, 92–96. https://doi.org/10.1111/j.1471-0528.1989.tb01582.x (1989).
35. Braustein, G. D., Buster, J. E., Soares, J. R. & Gross, S. J. Pregnancy hormone concentrations in marijuana users. *Life Sci.* **33**, 195–199. https://doi.org/10.1016/0024-3205(83)90413-7 (1983).
36. Nassan, F. L. et al. Marijuana smoking and outcomes of infertility treatment with assisted reproductive technologies. *Hum. Reprod.* **34**, 1818–1829. https://doi.org/10.1093/humrep/dez098 (2019).
37. Kaya, B. et al. Proliferation of trophoblasts and Ki67 expression in preeclampsia. *Arch. Gynecol. Obstet.* **291**, 1041–1046. https://doi.org/10.1007/s00404-014-3538-4 (2015).
38. Brooker, I. A., Fisher, J. J., Sutherland, J. M. & Pringle, K. G. Understanding the impact of placental oxidative and nitrative stress in pregnancies complicated by fetal growth restriction. *Placenta* **158**, 318–328. https://doi.org/10.1016/j.placenta.2024.11.005 (2024).
39. Walker, O. S. et al. Reactive oxygen species from mitochondria impacts trophoblast fusion and the production of endocrine hormones by syncytiotrophoblasts. *PLoS One*. **15**, e0229332. https://doi.org/10.1371/journal.pone.0229332 (2020).
40. Marín, R. et al. Oxidative stress and mitochondrial dysfunction in early-onset and late-onset preeclampsia. *Biochim. Biophys. Acta Mol. Basis Dis.* **1866**, 165961. https://doi.org/10.1016/j.bbadis.2020.165961 (2020).
41. Hu, Y. et al. Mitochondrial dysfunction and oxidative stress in selective fetal growth restriction. *Placenta* **156**, 46–54. https://doi.org/10.1016/j.placenta.2024.09.005 (2024).
42. El Marroun, H. et al. Intrauterine cannabis exposure affects fetal growth trajectories: the generation R study. *J. Am. Acad. Child. Adolesc. Psychiatry*. **48**, 1173–1181. https://doi.org/10.1097/CHI.0b013e3181bfa8ee (2009).
43. Kozlov, A. V., Javadov, S. & Sommer, N. Cellular ROS and antioxidants: physiological and pathological role. *Antioxid. (Basel)*. 13. https://doi.org/10.3390/antiox13050602 (2024).
44. LYONS, M. J., GIBSON, J. F. & INGRAM, D. J. Free-radicals produced in cigarette smoke. *Nature* **181**, 1003–1004. https://doi.org/10.1038/1811003a0 (1958).
45. Naserzadeh, P., Hosseini, M. J., Arbabi, S. & Pourahmad, J. A comparison of toxicity mechanisms of cigarette smoke on isolated mitochondria obtained from rat liver and skin. *Iran. J. Pharm. Res.* **14**, 271–277 (2015).
46. Li, G. et al. A mitochondrial specific antioxidant reverses metabolic dysfunction and fatty liver induced by maternal cigarette smoke in mice. *Nutrients* **11** https://doi.org/10.3390/nu11071669 (2019).
47. Sarafian, T. A. et al. Inhaled marijuana smoke disrupts mitochondrial energetics in pulmonary epithelial cells in vivo. *Am. J. Physiol. Lung Cell. Mol. Physiol.* **290**, L1202–1209. https://doi.org/10.1152/ajplung.00371.2005 (2006).
48. Wang, Y., Branicky, R., Noë, A. & Hekimi, S. Superoxide dismutases: dual roles in controlling ROS damage and regulating ROS signaling. *J. Cell. Biol.* **217**, 1915–1928. https://doi.org/10.1083/jcb.201708007 (2018).
49. Raja, A., Ahmadi, S., de Costa, F., Li, N. & Kerman, K. Attenuation of oxidative stress by cannabinoids and cannabis extracts in differentiated neuronal cells. *Pharmaceuticals (Basel)*. 13. https://doi.org/10.3390/ph13110328 (2020).
50. Singh, N., Hroudova, J. & Fisar, Z. Cannabinoid-Induced changes in the activity of electron transport chain complexes of brain mitochondria. *J. Mol. Neuroscience: MN*. **56**, 926–931. https://doi.org/10.1007/s12031-015-0545-2 (2015).
51. Sarafian, T. A., Kouyoumjian, S., Khoshaghideh, F., Tashkin, D. P. & Roth, M. D. Delta 9-tetrahydrocannabinol disrupts mitochondrial function and cell energetics. *Am. J. Physiol. Lung Cell. Mol. Physiol.* **284**, L298–306. https://doi.org/10.1152/ajplung.00157.2002 (2003).
52. Walker, O. S., Holloway, A. C. & Raha, S. The role of the endocannabinoid system in female reproductive tissues. *J. Ovarian Res.* **12**, 3. https://doi.org/10.1186/s13048-018-0478-9 (2019).
53. Sun, X. et al. Endocannabinoid signaling directs differentiation of trophoblast cell lineages and placentation. *Proc. Natl. Acad. Sci. U S A.* **107**, 16887–16892. https://doi.org/10.1073/pnas.1010892107 (2010).

54. Sun, X. & Dey, S. K. Endocannabinoid signaling in female reproduction. *ACS Chem. Neurosci.* **3**, 349–355. https://doi.org/10.1021/cn300014e (2012).
55. Costa, M. A. et al. The endocannabinoid Anandamide affects the synthesis of human syncytiotrophoblast-related proteins. *Cell Tissue Res.* **362**, 441–446. https://doi.org/10.1007/s00441-015-2236-2 (2015).
56. Dutta, S., Selvam, B., Das, A. & Shukla, D. Mechanistic origin of partial agonism of tetrahydrocannabinol for cannabinoid receptors. *J. Biol. Chem.* **298**, 101764. https://doi.org/10.1016/j.jbc.2022.101764 (2022).
57. Lazenka, M. F. et al. Delta FosB and AP-1-mediated transcription modulate cannabinoid CB_1 receptor signaling and desensitization in striatal and limbic brain regions. *Biochem. Pharmacol.* **91**, 380–389. https://doi.org/10.1016/j.bcp.2014.07.024 (2014).
58. Maia, J. et al. Effects of cannabis tetrahydrocannabinol on endocannabinoid homeostasis in human placenta. *Arch. Toxicol.* **93**, 649–658. https://doi.org/10.1007/s00204-019-02389-7 (2019).
59. Shukla, V., Iqbal, K., Okae, H., Arima, T. & Soares, M. J. Effects of an Aryl hydrocarbon receptor ligand on human trophoblast cell development. *Hum. Reprod.* **40**, 1163–1172. https://doi.org/10.1093/humrep/deaf075 (2025).
60. Li, H., van Ravenzwaay, B., Rietjens, I. M. & Louisse, J. Assessment of an in vitro transport model using bewo b30 cells to predict placental transfer of compounds. *Arch. Toxicol.* **87**, 1661–1669. https://doi.org/10.1007/s00204-013-1074-9 (2013).
61. Orendi, K., Gauster, M., Moser, G., Meiri, H. & Huppertz, B. The choriocarcinoma cell line bewo: syncytial fusion and expression of syncytium-specific proteins. *Reproduction* **140**, 759–766. https://doi.org/10.1530/REP-10-0221 (2010).
62. Brown, A. K. et al. Validated quantitative cannabis profiling for Canadian regulatory compliance - Cannabinoids, aflatoxins, and terpenes. *Anal. Chim. Acta*. **1088**, 79–88. https://doi.org/10.1016/j.aca.2019.08.042 (2019).
63. Cantwell, H. (2025).
64. Lan, R. et al. Design and synthesis of the CB1 selective cannabinoid antagonist AM281: a potential human SPECT ligand. *AAPS PharmSci.* **1**, E4. https://doi.org/10.1208/ps010204 (1999).
65. Ford, W. R., Honan, S. A., White, R. & Hiley, C. R. Evidence of a novel site mediating anandamide-induced negative inotropic and coronary vasodilatator responses in rat isolated hearts. *Br. J. Pharmacol.* **135**, 1191–1198. https://doi.org/10.1038/sj.bjp.0704565 (2002).

Acknowledgements
We are grateful to Dr. M Tarnopolsky and Dr. Joshua P Nederveen for providing the Seahorse XF. We also thank the Michael DeGroote Centre for Medicinal Cannabis Research for funding support for CM.

Author contributions
C.M., S.R., A.C.H. conceptualized the study; C.M., S.R., A.C.H., G.T.T. contributed to experimental design; C.M., T.P., G.T.T., M.M., J.P.N. A.M.L., T.T. conducted experiments and formal analysis; C.M., S.R., M.M., J.P.N, interpreted the data; C.M., T.P., A.C.H., S.R., writing – original draft preparation, C.M., T.P., M.M., J.P.N., A.M.L., T.T., G.T.T., A.C.H., S.R. reviewed and edited the manuscript. All authors reviewed and approved the manuscript.

Declarations

Competing interests
The authors declare no competing interests.

Additional information
Supplementary Information The online version contains supplementary material available at https://doi.org/10.1038/s41598-026-36939-8.

Correspondence and requests for materials should be addressed to S.R.

Reprints and permissions information is available at www.nature.com/reprints.

Publisher's note Springer Nature remains neutral with regard to jurisdictional claims in published maps and institutional affiliations.